Transportation Research Part C 40 (2014) 160–178

Contents lists available at ScienceDirect

Transportation Research Part C

journal homepage: www.elsevier.com/locate/trc

Probe vehicle based real-time traffic monitoring on urban roadways

Yiheng Feng *, John Hourdos, Gary A. Davis

Department of Civil Engineering, University of Minnesota, 500 Pillsbury Drive SE, Minneapolis, MN 55455, United States

ARTICLE INFO

Article history:
Received 30 April 2013
Received in revised form 14 October 2013
Accepted 20 January 2014

Keywords:
Arterial travel time estimation
Probe vehicle
Mixture normal distribution
Bayesian inference
Real-time traffic monitoring

ABSTRACT

Travel time estimation and prediction on urban arterials is an important component of Active Traffic and Demand Management Systems (ATDMS). This paper aims in using the information of GPS probes to augment less dynamic but available information describing arterial travel times. The direction followed in this paper chooses a cooperative approach in travel time estimation using static information describing arterial geometry and signal timing, semi-dynamic information of historical travel time distributions per time of day, and utilizes GPS probe information to augment and improve the latter. First, arterial travel times are classified by identifying different travel time states, then link travel time distributions are approximated using mixtures of normal distributions. If prior travel time data is available, travel time distributions can be estimated empirically. Otherwise, travel time distribution can be estimated based on signal timing and arterial geometry. Real-time GPS travel time data is then used to identify the current traffic condition based on Bayes Theorem. Moreover, these GPS data can also be used to update the parameters of the travel time distributions using a Bayesian update. The iterative update process makes the posterior distributions more and more accurate. Finally, two comprehensive case studies using the NGSIM Peachtree Street dataset, and GPS data of Washington Avenue in Minneapolis, were conducted. The first case study estimated prior travel time distributions based on signal timing and arterial geometry under different traffic conditions. Travel time data were classified and corresponding distributions were updated. In addition, results from the Bayesian update and EM algorithm were compared. The second case study first tested the methodologies based on real GPS data and showed the importance of sample size. In addition, a methodology was proposed to distinguish new traffic conditions in the second case study.

1. Introduction

Travel time is a crucial variable both in traffic demand modeling and network performance measurement. Today, travel time estimation and prediction on urban arterials is an important component of Active Traffic and Demand Management Systems (ATDMS). Although great progress has been achieved in ATDMS, reliable and efficient estimation of travel time is still not a wide spread accomplishment especially on arterials since it requires extensive sensor infrastructure normally found only on freeways.

* Corresponding author. Present address: Department of Systems and Industrial Engineering, The University of Arizona, 1127 E. James E. Rogers Way, P.O. Box 210020, Tucson, AZ 85721, United States. Tel.: +1 520 248 3988.

E-mail addresses: yihengfeng@email.arizona.edu (Y. Feng), hourd001@umn.edu (J. Hourdos), drtrips@umn.edu (G.A. Davis).

http://dx.doi.org/10.1016/j.trc.2014.01.010
0968-090X/

Several analytical models (Spiess, 1990; Xie et al., 2001; Skabardonis and Dowling, 1997; National Research Council, 2010; Bureau of Public Roads, 1964) have been proposed to relate arterial link travel time to traffic volume. Even with signal timing and volume information, these models can only provide the average travel time for all vehicles and are generally used in planning applications. In reality, different cluster of vehicles' travel time behave very differently. The average value couldn't reflect different components of travel time. Therefore, a travel time distribution, from which performance measures such as the mean travel time, or the standard deviation can be derived, is preferred.

In order to estimate the arterial travel time distribution, travel time information for individual vehicles is required. One feasible way to collect travel time data is from the monitoring systems. In the United States, most urban freeways are now equipped with sensor systems that allow real time monitoring of traffic conditions as well as estimating travel times. For urban arterial systems however the ability to monitor traffic conditions and estimate travel times has lagged behind. This is in large part due to the complexity of urban traffic environment.

These difficulties have led to an active interest in monitoring urban arterials using already-deployed sensors. One interesting possibility is to use probe vehicles. Certain types of vehicles, such as taxies or buses, which are easier to monitor, have been suggested as probe vehicles (Daily and Cathey, 2002). However, using special purpose vehicles has disadvantages. Buses have to stop at each bus stop, which overestimates travel times, while taxis behave differently when they are empty or full. Recently, the increasing availability of vehicles which can access the Global Positioning System (GPS) and the development of wireless telecommunication technologies, have permitted general road users to serve as probes. In principle, a steadily increasing number of GPS-equipped vehicles could lead to reliable, accurate travel time. Information transmitted from those GPS probe vehicles not only can help calculate travel time distributions on arterials, but also provides real-time traffic condition information.

The main difficulty with reliance on GPS probes is that the travel time provided by a single probe is essentially a sample, of size one, from the prevailing distribution of travel times. This leads to questions regarding the density of probes needed to produce useful sample sizes. Current, GPS equipped vehicle density is quite low and moreover one GPS vehicle could only provide information regarding one component of travel time at each link. Therefore, rather than attempt to estimate the travel time distribution from scratch, it may be possible to combine limited information from GPS probes with prior knowledge from signal timing and arterial geometry information to reconstruct the travel time distribution.

In this paper, a cooperative approach is chosen for travel time estimation using static information describing arterial geometry and signal timing information, semi-dynamic information of historical travel time distributions per time of day, and utilizes GPS probe information to augment and improve the latter. The objectives of this study focused on developing a methodology to characterize arterial travel time patterns by travel time distributions, propose methods for estimating such distributions from static information and refining them with the use of historical GPS probe information, and given such time and location based distribution use real-time GPS probe information to monitor arterial traffic conditions.

The rest of the paper is organized as follows: Section 2 provides a brief literature review in travel time estimation models. Section 3 introduces the NGSIM data used in this study and characterizes the travel time patterns on signalized arterial links by travel time states. Section 4 presents two approaches to estimate travel time distributions. In Section 5, two applications that combine travel time distributions with GPS data are illustrated. Sections 6 and 7 provide two comprehensive case studies using the NGSIM Peachtree Street (Atlanta, GA) dataset and Washington Avenue (Minneapolis, MN) GPS data. Section 8 concludes this paper and lays out the directions for further research.

2. Literature review

Estimation and prediction of arterial travel time has been one of the most popular topics in transportation engineering for decades. Zhang et al. (1997) summarized the early arterial travel time estimation models. He divided them into five different categories: Regression-type link travel time models (Gault, 1981; Young, 1988), Dynamic input–output link travel time models (Strobel, 1977), Sandglass link travel time models (Usami et al., 1986; Geroliminis and Skabardonis, 2006), Link travel time estimation based on pattern matching (Boehnke and Pfannerstill, 1986) and BPR-type model (Bureau of Public Roads, 1964; National Research Council, 2010). However, these BPR types of models tend to produce unreliable estimation under oversaturation conditions.

Probe vehicles are also used widely in travel time estimation. Daily and Cathey (2002) used a mass transit system as a speed sensor. This approach requires a "transit database" which contains the schedule times and geographical layout of every route and time point. In addition, all the transit vehicles used as probes should be equipped with a transmitter such as GPS receiver, and report back to control center periodically. Liu and Ma (2009) proposed a virtual probe vehicle method for arterial travel time estimation. A virtual probe is a simulated vehicle that is released from the origin to the destination at certain time point. This approach actually used data from loop detectors rather than real probe vehicles. Bluetooth devices were also equipped in vehicles to acquire individual travel times (Hainen et al., 2011). When the Bluetooth equipped vehicle passes the upstream/downstream detection points, the MAC address of the Bluetooth device is recorded. The travel times were then collected by matching the MAC addresses. Herrera et al. (2010) collected data from GPS-enabled Nokia N95 phones to estimate travel time. They claimed that a 2–3% penetration of cell phones in the driver population was enough to provide accurate measurement. In the following research (Hunter et al., 2009), travel time distributions were extracted from raw GPS measurements and presented the arterial network by a probabilistic model with expectation maximization

(EM) algorithm for learning the parameters. One limitation of their work was that they assumed the link travel times were independent. In reality, there are strong correlations between link travel times.

3. Characterization of travel time patterns

In order to better illustrate the travel time characteristics, the NGSIM data used throughout the paper is introduced first.

3.1. Data introduction

As part of the NGSIM (FHWA, 2006) program, detailed traffic data were collected on a segment of Peachtree Street, in Atlanta Georgia, on November 8th, 2006 (Cambridge Systematics Inc., 2007). This arterial segment is approximately 2,100 feet in length, with five intersections and two or three through lanes in each direction. The segment is divided into six links, numbered from one to six running from south to north, bounded by the neighboring intersections. Links 1 and 6 turned out to be too short for useful analysis, so our study area is limited to links 2 through 5. Four of the five intersections are signalized, with intersection 4 being un-signalized. Fig. 1 shows the geometric structure of the study area. The Peachtree Street data consist of two 15-min time periods, 12:45 p.m. to 1:00 p.m. and 4:00 p.m. to 4:15 p.m. These two periods were taken to represent two different traffic conditions, which we call "Noon" and "PM".

The data includes detailed individual vehicle trajectories with time and location stamps, from which the link travel times of individual vehicles can be calculated. In this study, link travel time refers to the time a vehicle enters the arterial link to the time this vehicle passes the stop-bar at the end of the link. Travel time through on intersection is excluded.

3.2. Characterization of travel times on a signalized arterial link

Travel time patterns on signalized arterial links can vary in complexity under different situations. The main factors that affect travel time patterns on an arterial roughly fall into the following four categories:

- Geometric structure of the arterial including link length, number of lanes, speed limit, roadway alignment, and driveways.
- Driving behavior, including lane changing rate, car following behavior and driver aggressiveness.
- Signal control strategy including cycle length, phase splits, effective green time and offsets.
- Traffic demand such as traffic volume of the main arterial, the turning movement flows at the intersections, and the volume ratio between main arterial and the side streets.

Other factors which are not considered in this study include the presence of buses and availability of pull offs, presence of pedestrians, driveways along the arterial etc.

For a given location, over the course of the day it is reasonable to think that the geometric structure of the arterial is unchanged and the driving behavior remains similar, leaving the traffic demand and signal control as the determinants of travel time. That is, under one specific traffic condition (combination of signal control strategy and given traffic demand level/pattern), it is assumed that the travel time distributions are similar. As a result, a set of different travel time distributions are needed for different combinations of demand and signal timing.

Fig. 2(a) shows a typical travel time histogram for a signalized arterial link from the NGSIM Peachtree Street dataset (Link 2 Northbound at Noon). This histogram shows the travel time of vehicles which go through to the downstream link. Different colors in the figure represent the different origins of the vehicles. For example, green[1] vehicles come from the through direction of the upstream intersection while brown and grey vehicles come from the side streets of the upstream intersection. It can be seen that travel times of green vehicles cluster around 10 s and 70 s, and that travel times of grey and brown vehicles tend to fall between those of green vehicles. Apparently, travel times from different origins are different due to different encounters with the different phases of signal control.

Focusing attention to through–through vehicles, defined as vehicles traveling through from the upstream boundary to the downstream, as shown in Fig. 2(b), gives a clear two-peak pattern as well as several additional travel time points located between the two peaks or beyond the second peak. The two peaks are the major components of travel time, representing non-stopped vehicles and stopped vehicles. Non-stopped vehicles refer to vehicles which pass the end of the link without stopping, while stopped vehicles refer to vehicles stopping at the end of the link for a red signal. The scattered points between the two peaks or beyond the second can be recognized as two additional components: non-stopped with delay and stopped with delay, where the additional delay is not caused by the signal control, but by some "incidents". For example, some through vehicles can be delayed by a preceding vehicle making a permitted right turn or left turn. Other reasons such as slow moving vehicles, violating the traffic rule, or vehicles entering or exiting from driveways can also cause such delays.

In this paper, we will restrict attention to through–through vehicles and use the phrase travel time states to represent different travel time components. In short, four states of travel time are defined:

[1] For interpretation of color in Figs. 2, 5, 7, 9, 10, 11, 14 and 15, the reader is referred to the web version of this article.

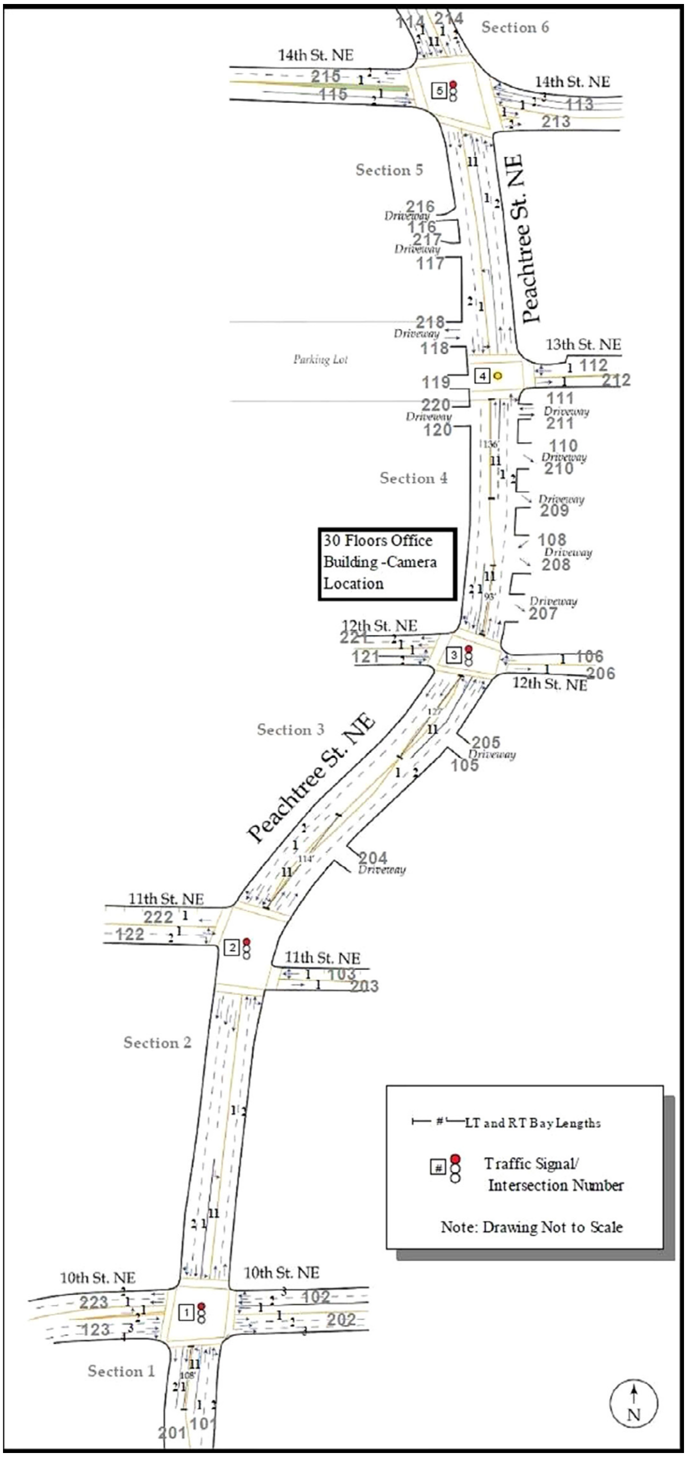

Fig. 1. NGSIM Peachtree Street Dataset geometry. *Source:* NGSIM Peachtree Street (Atlanta) Data analysis report (Cambridge Systematics, 2007).

- State 1: non-stopped.
- State 2: non-stopped with delay.
- State 3: stopped.
- State 4: stopped with delay.

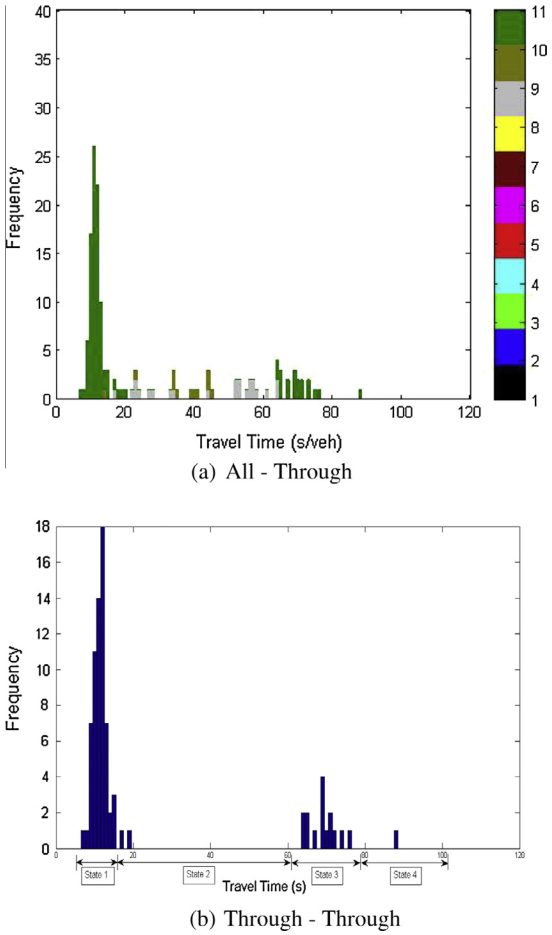

Fig. 2. Travel time histograms of link 2 Northbound at Noon (Peachtree St).

Vehicles that make turns at the end of the intersection or vehicles from minor streets may have different states. The travel time patterns involving turning vehicles are therefore much more complicated than through–through vehicles. For right turning vehicles, usually right turn can be made when the signal is red and sometimes there is no separate right turn bay. For left turning vehicles, similar geometry issues may apply and sometimes the left turn signal is divided into protected and permitted intervals. Both left turning and right turning vehicles are required to yield to through traffic. Those complexities make it much more difficult to analyze the travel time patterns of turning vehicles. Moreover, through–through vehicles are usually the main component of the total traffic. Therefore, for simplicity, in this paper, only through–through vehicles are taken into consideration.

4. Estimation of travel time distributions

4.1. Estimation with Expectation–Maximization (EM) algorithm

Section 3 stated that the travel time histogram for through–through vehicle follows a two-peak pattern. Therefore, a bi-modal distribution could be used to fit the travel time histogram in state 1 and state 3. Empirical characterization of travel time distributions on signalized arterials shows that this bimodal distribution can be approximated using a mixture of normal densities (Davis and Xiong, 2007; Xiong and Davis, 2009) as shown in Eq. (1).

$$f(TT) = p \times f_n(TT) + (1 - p) \times f_s(TT) \quad (1)$$

where, p is the portion of non-stopped vehicles.

$f_n(TT)$ is the *pdf* for non-stopped vehicles (first peak), which follows a normal distribution with mean μ_1 and variance σ_1^2, and $f_s(TT)$ is the *pdf* for stopped vehicles (second peak), which follows a normal distribution with mean μ_2 and variance σ_2^2.

Given the travel time of a specific vehicle, it is unknown whether it belongs to non-stopped vehicles or stopped vehicles. The travel times are then grouped into m intervals, where $m = round(TT_{max} - TT_{min}) + 1$. Consequently, the width of each interval is 1 s. Assume $n_1 \ldots n_m$ are the number of travel times that falls into intervals $[a_0, a_1], \ldots, [a_{m-1}, a_m]$.

Let ψ denotes the parameter set $(p, \mu_1, \sigma_1^2, \mu_2, \sigma_2^2)$. Then the probability that an individual vehicle travel time falls in the jth interval is given by:

$$P_j(\psi) = \int_{a_{j-1}}^{a_j} f(TT|\psi)dTT, \quad j = 1, \ldots, m \tag{2}$$

The grouped data then follow a multinomial distribution with likelihood function

$$L(\psi) = \frac{n!}{n_1! \ldots n_m!} \{P_1(\psi)\}^{n_1} \ldots \{P_m(\psi)\}^{n_m} \tag{3}$$

and the log-likelihood function is

$$\log L(\psi) = \sum_{j=1}^{m} n_j \log(P_j(\psi)) + \log\left(\frac{n!}{n_1! \ldots n_m!}\right) \tag{4}$$

Maximum likelihood estimates of mixture model parameters can be accomplished using the expectation–maximization (EM) algorithm (McLachlan and Krishnan, 2008). This is accomplished using the R software package mixdist (Du, 2002).This routine uses the standard maximum likelihood estimation method and combines the EM algorithm with a Newton-type method.

Figs. 3 and 4 show the estimated travel time distributions (normal mixture) of state 1 and state 3 for links 2 to 5, under two traffic conditions Noon and PM of the Peachtree Street dataset. As mentioned above, intersection 4 is an un-signalized intersection, and left turns at intersection 4 were forbidden, so link 4 and link 5 were treated as one single link, yielding three consecutive links. Note that all travel time distributions show that the traffic conditions are not oversaturated. Under oversaturated traffic conditions, the distribution may have a third peak representing vehicles in the residual queue (stopped

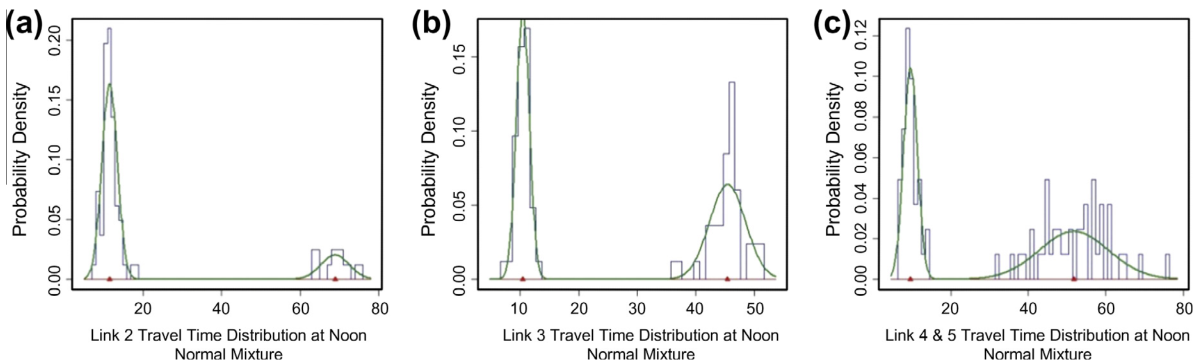

Fig. 3. Normal mixture approximation of travel time state 1 and 3 at Noon.

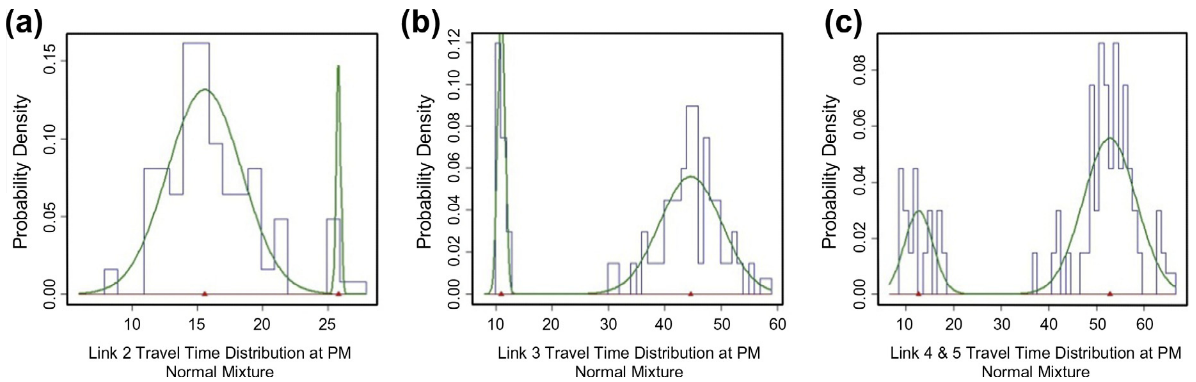

Fig. 4. Normal mixture approximation of travel time state 1 and 3 at PM.

twice). The EM algorithm could also be applied to oversaturated traffic conditions where the travel time distributions have more than two components.

The mixture distributions in Fig. 3 and Fig. 4 only represent stopped and non-stopped components, which are vehicles in state 1 and state 3. Since the number of observations in state 2 and state 4 is small, it is difficult to identify a unimodal distribution for these. So it is assumed that the probabilities of delay times caused by different 'incidents' in state 2 and state 4 are equally likely, which suggests travel times in state 2 or state 4 follow uniform distributions. The upper boundary and lower boundary of these two uniform distributions can be approximated as follows. Suppose the non-stopped component is normally distributed with mean and variance μ_1 and σ_1^2 while the stopped component is normally distributed with mean and variance μ_2 and σ_2^2. If an observed travel time is located beyond $\mu_1 + 3\sigma_1$ which is approximately the 99th percentile for the state 1, then it is reasonable to think that this travel time does not belong to state 1, and $\mu_1 + 3\sigma_1$ is considered as the lower boundary of the uniform distribution for state 2 (non-stopped with delay). Based on this rule, the upper boundary for non-stopped with delay, and the lower boundary for stopped with delay can be defined. The upper boundary for state 4 (stopped with delay) is assumed not to exceed a certain value TT_{max} which is the longest possible travel time in one arterial link. The longest travel time can be estimated from historical data when the arterial link was congested.

4.2. Estimation based on signal control and geometry

The previous section described how to estimate a travel time distribution based on individual vehicle travel times. However, under many circumstances, travel times of individual vehicles are not readily available. As an alternative, this section proposes an approach to compute travel time distributions for state 1 and state 3 based on the signal control and arterial geometry.

Some assumptions are made to simplify the problem. First, the signals of upstream and downstream intersections are coordinated, which means that the signals should have the same cycle length. Second, queues can be fully discharged during one cycle so that non-oversaturated traffic condition applies. Third, the turning rate from side streets is negligible. This assumption assures that vehicles from side streets should not affect the travel time on the main arterial too much.

Given these assumptions, if the travel time distribution for state 1 and state 3 can be approximated using mixture of normal densities, as shown in Equation (1), then five parameters $(\mu_1, \sigma_1^2, \mu_2, \sigma_2^2, p)$ need to be estimated.

- Estimation of μ_1

μ_1 is the mean travel time of non-stopped vehicles, which can be considered as free flow travel time. It can be initially estimated by link length and speed limit:

$$\mu_1 = L/V_L \tag{5}$$

where, L is the link length, and V_L is the speed limit of the arterial link.

- Estimation of σ_1

σ_1 is the standard deviation of the free flow travel time. Unfortunately, there is not a priori way to estimate the standard deviation of travel time without data. However, since travel time is the reciprocal of speed, given a link length, σ_1 could be converted from the standard deviation of speed. Empirical studies suggest that standard deviation of speed varies a lot under different demands. For example, it shows a U-shape (Nezamuddin et al., 2009) relation with respect to traffic volume. That is, when either the traffic demand is low or high, the standard deviation increases. When the traffic demand is within intermediate ranges, the standard deviation remains low and stable. Existing literature (Box, 1976; Oppenlander, 1963) suggests a standard deviation of 5–7 mph for speed distribution, under intermediate range of demand.

- Estimation of μ_2 and σ_2

μ_2 and σ_2 are mean travel time and standard deviation of stopped vehicles, which are closely related to the signal settings of the upstream and downstream intersections.

By assumption, the travel time of stopped vehicles also follows a normal distribution. According to the properties of normal distribution, if one wants to estimate the mean and standard deviation, instead of estimating directly, one could estimate the lower and upper boundary of 99th percentile, and then calculate the mean and standard deviation accordingly. Suppose the lower and upper boundary of the 99th percentile are a and b respectively. Then by the symmetry property, the mean could be calculated as $\mu = (a + b)/2$. Moreover, the distance from the mean to the 99th percentile is 3σ. Therefore, standard deviation could be calculated as $\sigma = (b - \mu)/3$ or $\sigma = (\mu - a)/3$.

The 99th percentile of link travel time can be estimated by adding the upper and lower boundary of total delay to free flow travel time.

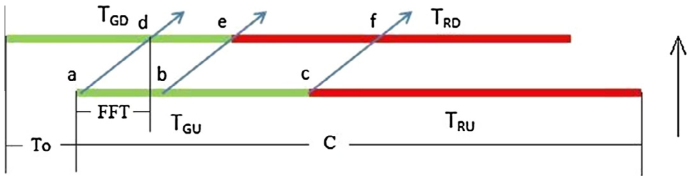

Fig. 5. Time–space diagram for two consecutive intersections.

To estimate upper and lower boundary of signal delay, we need to know the signal control plan such as cycle length, green and red split and the offset between upstream and downstream intersections. An example time–space diagram of two consecutive intersections is shown in Fig. 5. The arrow on the right is the movement direction.

Where, $\mathbf{T_{GD}}$ and $\mathbf{T_{RD}}$ are the green/red time of downstream intersection.

- $\mathbf{T_{GU}}$ and $\mathbf{T_{RU}}$ are the green/red time of upstream intersection.
- **C** is the cycle length.
- **To** is the offset between two signals.
- **FFT** is the non-stopped vehicle mean travel time (equal to μ_1).

By looking at the time–space diagram, one can easily see that vehicles pass during $\mathbf{T_{GD}}$ are non-stopped vehicles while vehicles reach the downstream intersection during $\mathbf{T_{GD}}$ are stopped vehicles. The estimation of the upper and lower boundaries of signal delay can be categorized into the follow three cases:

Case I $\mathbf{To} + \mu_1 < \mathbf{T_{GD}} < \mathbf{To} + \mathbf{T_{GU}} + \mu_1$

$$D_{\text{upper}} = T_{RD} \quad D_{\text{lower}} = C - (To + T_{GU} + \mu_1)$$

Case II $\mathbf{T_{GD}} < \mathbf{To} + \mu_1$

$$D_{\text{upper}} = C - (To + \mu_1)$$

$$\text{if } To + T_{GU} + \mu_1 < C \rightarrow D_{\text{lower}} = C - (To + T_{GU} + \mu_1)$$

$$\text{if } To + T_{GU} + \mu_1 > C \rightarrow D_{lower} = 0$$

Case III $\mathbf{T_{GD}} > \mathbf{To} + \mathbf{T_{GU}} + \mu_1$

$$D_{\text{upper}} = 0 \quad D_{\text{lower}} = 0$$

where, D_{upper} and D_{lower} are upper and lower boundaries of signal delay.

In case I, where $\mathbf{To} + \mu_1 < \mathbf{T_{GD}} < \mathbf{To} + \mathbf{T_{GU}} + \mu_1$, the green red split at the downstream intersection is between the green time start of the upstream intersection plus the free flow travel time, and the green time end of upstream intersection plus free flow travel time. That is, point *e* is between point *a* and point *c* in Fig. 5. Suppose vehicle 1 passes the upstream intersection at point *b* and arrives at the downstream intersection at the beginning of the red signal (point *e*). Since there is no residual queue from the previous cycle, vehicle 1 must be the first in the queue and thus would not experience extra queue discharging time. Then the longest signal delay time is considered as the duration of red signal at the downstream intersection. Suppose vehicle 2 passes the upstream intersection at time point *c* and arrives at the downstream intersection at time point f. Its signal delay time is from time point f until the end of red signal at the downstream intersection. Only if no vehicle passes the upstream intersection between time point *b* and *c*, would vehicle 2 be the only vehicle in the queue. Otherwise, vehicle 2 would experience extra queue discharging delay. So the shortest delay time is considered as the length of the red time from the time point when vehicles which passed the upstream intersection at the end of the green time arrive at the downstream intersection to the end of red signal (from point f to the end of G_{RD}). Cases II and III are analyzed similarly.

Therefore the lower and upper boundary of the 99th percentile of travel time can be approximated as:

$$TT_{\text{upper}} = D_{\text{upper}} + \mu_1 + 3\sigma_1 + T_R \tag{6}$$

$$TT_{\text{lower}} = D_{\text{lower}} + \mu_1 - 3\sigma_1 + T_R \tag{7}$$

where, TT_{upper} and TT_{lower} are the upper and lower boundary of travel time respectively, and T_R is the start up delay.

Since $\mu_1 + 3\sigma_1$ is the upper boundary of 99th percentile free flow travel times and travel time of stopped vehicles could be treated as free flow travel time plus delay time. Therefore, TT_{upper} could also be considered as the upper boundary of 99th percentile of travel time for the stopped vehicles. For the same reason, TT_{lower} is the lower boundary of 99th percentile of travel time.

Then, μ_2 and σ_2 can be calculated as:

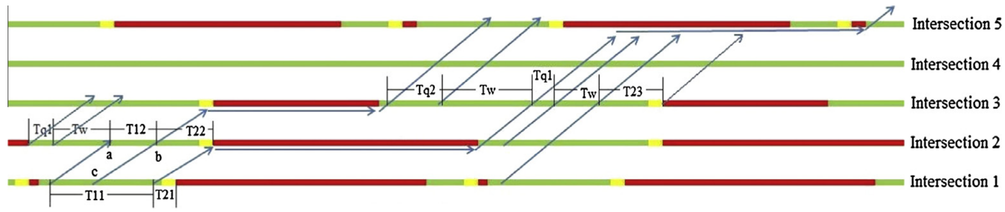

Fig. 6. Example on estimation of p.

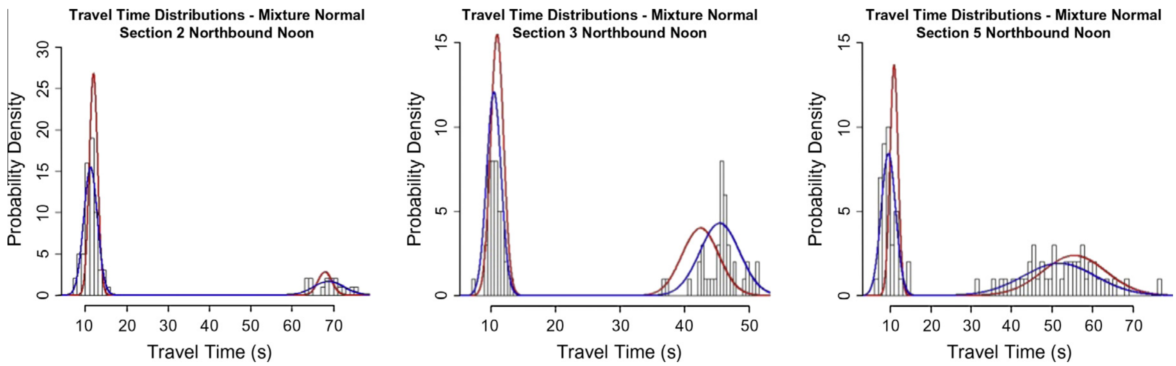

Fig. 7. Comparison, EM algorithm and estimation from signal timing and geometry.

$$\mu_2 = (TT_{\text{upper}} + TT_{\text{lower}})/2 \tag{8}$$

$$\sigma_2 = (\mu_2 - TT_{\text{lower}})/3 \text{ or } \sigma_2 = (TT_{\text{upper}} - \mu_2)/3 \tag{9}$$

- Estimation of p

Since the parameter p is the proportion of non-stopped vehicles and $1 - p$ is the proportion of stopped vehicles, it can be estimated by combining the signal timing information and arrival rate at the entrance of the corridor, as shown in Fig. 6.

Suppose Intersection 1 is the entrance of the corridor. Based on the time–space diagram and the free flow speed (shown as the slope of the arrows), vehicles passing Intersection 1 during T_{11} are non-stopped vehicles while vehicles pass during T_{21} are stopped vehicles. Let the average arrival rates (veh/s) during T_{11} and T_{21} be q_1 and q_2 respectively. The average arrival rate could be obtained for example from loop detectors at the stop bar. Therefore the number of non-stopped vehicles on the link between Intersection 1 and Intersection 2, $N_{11} = T_{11} \times q_1$, and the number of stopped vehicles $N_{21} = T_{21} \times q_2$. Then ratio of the first link $p_1 = N_{11}/(N_{11} + N_{21})$.

The situation gets more complicated when calculating the ratio for the second link. The vehicles pass during T_{21} become a queue at Intersection 2. When the signal turns green at Intersection 2, it takes time T_{q1} to discharge the queue which is propagated during T_{21}. As a result, stopped vehicles in link 1 become non-stopped vehicles in link 2. After the queue is fully discharged, there is a period of time T_w when no vehicles pass Intersection 2 because the next platoon from intersection 1 will not arrive at Intersection 2 until time point T_a. So vehicles which pass Intersection 2 between time point T_a and time point T_b (time interval T_{12}) are non-stopped vehicles while vehicles passing Intersection 2 between time point T_b and the green time end (time interval T_{22}) are stopped vehicles. The total number of non-stopped vehicles in link 2, say, N_{12} is equal to number of vehicles passing during T_{q1} and T_{12}. So $N_{12} = N_{21} + T_{12} \times q_1$. The number of stopped vehicles of link 2, $N_{22} = T_{22} \times q_1$. Then ratio of non-stopped vehicles at link 2, $p_2 = N_{12}/(N_{12} + N_{22})$. The subsequent links are analyzed in a similar way.

Different signal settings and different offsets will result in different scenarios. For example, there are two periods of unused green time T_w at intersection 3. However, the analysis technique is the same and can be applied to most real world situations.

Fig. 7 shows a comparison of travel time distributions estimated from signal timing and geometry (red curve) and from data using EM algorithm (blue curve). The NGSIM Peachtree Street Dataset noon traffic condition was used for the test (Link 2, 3 and 5 from left to right). Although the estimation of some parameters, such as the mean of the second peak in Link 3, is not very accurate, they are good enough for a prior distribution for further updating. A detailed description of how to update travel time distributions will be given in Section 5.2.

5. Applications of travel time distribution

Travel time distributions provide a range of performance measures, such as mean travel time, the standard deviation, and the 95th percentile travel time. Meanwhile, GPS data offer information of individual vehicle information in real-time. Useful information can be derived combining travel time distribution and GPS data. This section describes how the prevailing actual traffic conditions can be identified in real-time. The same methodology is also used to update the parameters of travel time distributions for the most fitting time period preventing abnormal conditions from distorting the distributions.

5.1. Real-time traffic condition identification

Figs. 3 and 4 show that the travel time distributions of each link under different traffic conditions are also different. In Consequence, traffic conditions could be differentiated by the travel time distributions of each link. When a GPS probe vehicle goes through a certain route, it records travel time of each individual link at that time. In principle, given that a number of unexpected events can disrupt normal traffic conditions, it is unknown which is the actual prevailing traffic condition. Therefore, it is important to identify the prevailing conditions for what they represent regardless of the actual time of day the data were collected. This way we can identify abnormal traffic conditions (accident, special event, etc.), as well as select the appropriate control strategy if these conditions are similar to ones regularly observed during other times of the day. Given characterization of two traffic conditions, Bayes theorem can be used to compute posterior probabilities that a given travel time sequence belongs to a traffic condition.

Either the travel time distribution of the whole route or the travel time distribution of each link can be used to classify the GPS data. Using the travel time of the whole route is a more direct way. However, it is more feasible to use travel time distribution of every single link because then the route could be constructed freely as long as the relationship between links can be found. In addition, under different traffic conditions, the travel time distribution of the whole route could be similar, even though the travel time distributions of single links differ. Therefore, in this study, link travel time distributions are used.

Suppose an arterial route consists of n consecutive links, and a sequence of link travel times is collected from a GPS vehicle running along this route. Let S_i and T_i denote travel time state and travel time of link i respectively. The joint probability of travel time states could be expressed by the following equation.

$$P(S_1 = s_1, S_2 = s_2, \ldots, S_n = s_n) = P(S_n = s_n | S_{n-1} = s_{n-1}, \ldots, S_2 = s_2, S_1 = s_1) \times P(S_{n-1} = s_{n-1} | S_{n-2} = s_{n-2}, \ldots, S_2 = s_2, S_1 = s_1) \times \cdots \times P(S_2 = s_2 | S_1 = s_1) \times P(S_1 = s_1) \tag{10}$$

Assuming the travel time of a single link is conditionally independent of travel time states on other links:

$$P(T_i = t_i | S_1 = s_1, S_2 = s_2, \ldots, S_i = s_i, \ldots, S_n = s_n) = P(T_i = t_i | S_i = s_i) \tag{11}$$

Combined with Eqs. (10) and (11), the join distribution of travel time and travel time states can be seen in Eq. (12).

$$P(T_1 = t_1, \ldots, T_n = t_n, S_1 = s_1, \ldots, S_n = s_n) = \left(\prod_{i=1}^{n} P(T_i = t_i | S_i = s_i) \right) P(S_1 = s_1, \ldots, S_n = s_n) \tag{12}$$

The marginal distribution for travel times then becomes

$$P(T_1 = t_1, \ldots, T_n = t_n) = \sum_{S_1 = s_1, \ldots, S_n = s_n} \left(\prod_{i=1}^{n} P(T_i = t_i | S_i = s_i) \right) P(S_1 = s_1, \ldots, S_n = s_n) \tag{13}$$

The joint probability of travel time states $P(S_1 = s_1, \ldots, S_n = s_n)$ could be estimated from the observed travel time states of each GPS vehicle at each link.

Assuming there are m different traffic conditions, the probability that a given travel time sequence belongs to traffic condition C_i can be calculated by Bayes theorem (DeGroot and Schervish, 2002).

$$P(C_i | T_1 = t_1, \ldots, T_n = t_n) = \frac{P(T_1 = t_1, \ldots, T_n = t_n | C_i) \times P(C_i)}{\sum_{j=1}^{m} P(T_1 = t_1, \ldots, T_n = t_n | C_j) \times P(C_j)} \tag{14}$$

Since the travel time distributions under every traffic condition are known, the likelihood $P(T_1 = t_1, \ldots, T_n = t_n | C_j)$ can be obtained from Eq. (13). The prior probability $P(C_j)$ can be flat or calculated from the traffic volume of each traffic condition. For example, in the NGSIM Peachtree St Dataset, there are two traffic conditions: noon and PM. 82 vehicles went through the route during the noon period and 67 vehicles during the PM period. If a vehicle is randomly picked, the probability it belongs to noon data set, which is $P(Noon) = 82/(82 + 67) = 0.55$. Consequently, $P(PM) = 1–0.55 = 0.45$. Then the marginal distribution of travel time under different traffic conditions $P(T_1 = t_1, T_2 = t_2, T_3 = t_3 | noon)$ and $P(T_1 = t_1, T_2 = t_2, T_3 = t_3 | PM)$ can be then calculated from travel time distributions.

Because currently GPS data of that arterial segment are not available, travel time data from the NGSIM Peachtree St Dataset are used to test the method. If it works well, vehicles from the Noon data set should have a high posterior probability of belonging to the noon traffic condition and a low probability of belonging to the PM traffic condition, and vice versa. Fig. 8 shows the results.

The dots on the left side of the vertical line are the vehicles from the noon data set and right side are the vehicles from the PM data set. One dot represents one vehicle. The figure shows that generally, data from a single GPS-equipped vehicle could be enough to discriminate between the two traffic conditions. Although the probabilities of a few dots on the left are low,

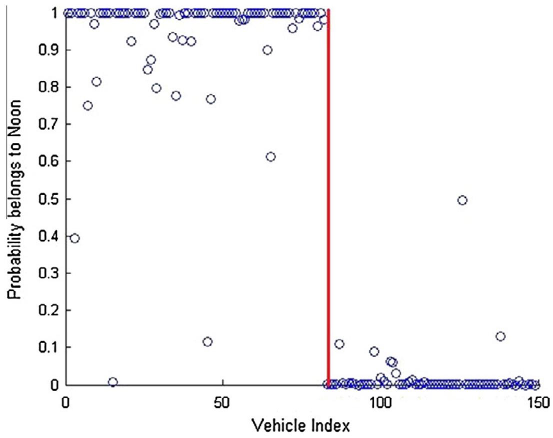

Fig. 8. Traffic condition identification of NGSIM Peachtree St Dataset.

most of them located around one. It is worth pointing out that the identification could be wrong (the other side) or vague (the probability is around 0.5). In that case, more than one GPS vehicle is needed to identify the traffic condition.

5.2. Travel time distribution parameter update

This section proposes an approach to update the parameters of the travel time distribution under a Bayesian scheme. To apply a Bayesian approach, a prior distribution must be chosen first. When no prior information is available, it is common to use a non-informative prior. It is usually a uniform distribution or a normal distribution with a large variance that has minimal impact on the posterior distribution. Many statisticians are in favor of non-informative priors because they appear to be more objective. But in some cases, non-informative priors can lead to improper posteriors. More importantly, in this case, even if the non-informative prior is a proper prior, given the density of the GPS probe vehicles is very low and spread into different traffic conditions, it might take a very long time to update to a good posterior distribution. Especially under traffic conditions such as off-peak hours when there are fewer GPS probes, the time would be even longer. Consequently, we considered travel time distributions estimated from signal timing and arterial geometry as prior distribution when no prior travel time data is available. Combining with GPS data, posterior distributions can then be calculated.

Unfortunately, the posterior distribution of a mixture normal density is analytically intractable (McLachlan and Peel, 2000). As a result, Markov Chain Monte Carlo (MCMC) simulation (Berg, 2004) is applied to estimate the posterior distribution. One particular sampling technique of Markov Chain called Gibbs sampling (Diebolt and Robert, 1994) is used. In this paper, WINBUGS ("BUGS" stands for Bayesian inference using Gibbs sampling) software is used to compute the posterior distributions. It performs Bayesian analysis of complex statistical models using MCMC methods (Lunn et al., 2013).

Notice that the mixture normal distribution consists of two unimodal normal distributions and the two normal components are connected by the ratio *p*. *p* follows a Bernoulli random variable, which captures the variations of the portions of the two components. For a unimodal normal distribution with unknown mean and variance, there is conjugate prior for the posterior distribution, given the data are *iid* normal.

The conjugate prior for a two parameter normal is the normal-inverse gamma distribution (Bernardo and Smith, 2000) with density

$$f(\mu,\sigma^2) = f(\mu|\sigma^2)f(\sigma^2)$$

where $f(\mu|\sigma^2) = N(\alpha_0, \beta_0)$ and $f(\sigma^2) = IG(\gamma_0, \delta_0)$, $IG(\gamma_0, \delta_0)$ is the inverse-gamma distribution with parameters γ_0, δ_0. Note that if $X \sim IG(\gamma_0, \delta_0)$, then $X^{-1} \sim Gamma(\gamma_0, \delta_0)$. Therefore, we replace σ^2 with precision $\lambda = 1/\sigma^2$. With this approach, the prior for the parameter (μ, λ) is a normal-gamma distribution, denoted by

$$f(\mu,\lambda) \sim NG(\alpha_0, \beta_0, \gamma_0, \delta_0)$$

Suppose the data (likelihood) are iid normal, $f(Y_i|\mu,\lambda) \sim N(\mu,\lambda) \sim i = 1, 2, \ldots, n$. Because of independence, the total likelihood is the product of each likelihood, denoted by $f(Y|\mu,\lambda) = \prod_{i=1}^{n} f(Y_i|\mu,\lambda)$. Suppose the sample mean is $\bar{y}$ and the sample variance is V_n. Then, the corresponding posterior distribution is also a normal-gamma distribution with parameters $(\alpha_1, \beta_1, \gamma_1, \delta_1)$.

$$f(\mu,\lambda|y) = f(Y|\mu,\lambda) \times f(\mu,\lambda) = NG(\alpha_1, \beta_1, \gamma_1, \delta_1)$$

where,

$$\alpha_1 = \alpha_0 + \frac{n_1}{2}, \quad \beta_1 = \beta_0 + \frac{n_1}{2}\left(V_n + \frac{\delta_0(\bar{y}-\gamma_0)^2}{\delta_0 + n_1}\right), \quad \gamma_1 = \frac{\gamma_0\delta_0 + n_1\bar{y}}{\delta_0 + n_1}, \quad \delta_1 = \delta_0 + n_1$$

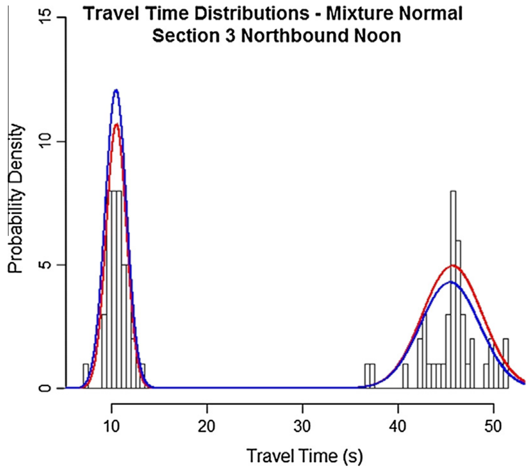

Fig. 9. Posterior travel time distribution.

Given the above structure, a hierarchical Bayesian model could be constructed in WINBUGS. The structure of the hierarchical model can be specified as below:

$Y_i|Pi,\ \lambda_{(\mathrm{Pi})},\ \mu_{(\mathrm{Pi})} \sim Normal(\mu_{(\mathrm{Pi})},\ \lambda_{(\mathrm{Pi})})$.
$\mu_{(\mathrm{Pi})}|Pi,\ \lambda_{(\mathrm{Pi})} \sim Normal(\varepsilon_{(\mathrm{Pi})},\ \delta_{(\mathrm{Pi})})$.
$\lambda_{(\mathrm{Pi})}|Pi \sim Gamma(\alpha_{(\mathrm{Pi})},\ \beta_{(\mathrm{Pi})})$.
$P_i \sim Bern(r)$ r: determined by ratio of non-stopped and stopped vehicles.

Some simulation experiments are run in WINBUGS to test the model. The number of Markov Chains is set to one. One simulation scenario includes 21,000 samples, in which the first 1000 samples are burn-in samples and the following 20,000 samples are used to create the posterior distribution. The posterior means of each parameter are selected to be the new parameters of the travel time distribution. Fig. 9 shows an example of the comparison between the posterior travel time distribution from Bayesian update (red curve) and travel time distribution directly estimated from EM algorithm (blue curve). In this example, same travel time data are used. One can see the two approaches lead to similar results because asymptotically Bayesian inference and classical maximum likelihood estimation should converge to the same distribution when the sample size is big enough.

6. A case study – NGSIM Peachtree Street Dataset

In previous sections, methods regarding for constructing travel time distribution and their applications were discussed. This chapter aims to connect these models together and demonstrate a comprehensive case study based on the NGSIM Peachtree dataset.

Suppose we are interested in estimating the travel time distributions of a given arterial under different traffic conditions. Usually the signal timing plans and the geometric structure of the arterial are known, but the travel time data are not available in the first place. As a result, instead of starting with flat prior, travel time distributions are estimated based on signal timing plans and arterial geometry (Section 4.2). When GPS data are collected for the targeted route, traffic condition identification process (Section 5.1) is run and the probability one particular data point belongs to every traffic condition is calculated. Data are then classified according to the posterior probabilities. Finally, a Bayesian update (Section 5.2) is run to calculate posterior distributions under each traffic condition combining with classified data. Furthermore, when new GPS data are available, the posterior distributions from the previous update are considered as new priors and the update process is repeated. As long as more and more GPS data become available, the posterior distribution would be more and more consistent with reality.

In the dataset, there are two traffic conditions: Noon and PM. We assume there is no prior travel time data under both traffic conditions and consider travel time data from vehicle trajectories as incoming GPS data. The total sample size of GPS data in two traffic conditions is 149 which are further divided into two parts in order to perform the update process iteratively. One GPS datum is one travel time sequence including the three link travel times in link 2, link 3 and link 5 respectively.

- Prior distributions

First, prior distributions were estimated from the signal timing and geometric properties of the arterial. Yellow curves in Fig. 10 and Fig. 11 show the prior distributions under traffic condition Noon and PM respectively.

• Data classification

The traffic condition identification process is then performed on the first half of the data (75 travel time sequences). Fig. 12(a) shows the posterior probabilities that each GPS vehicle belongs to Noon traffic condition.

The following criteria were applied to classify the data:

- If $P(belong\ to\ noon) \geqslant 0.7 \rightarrow$ use this data to update Noon travel time distribution.
- If $P(belong\ to\ noon) \leqslant 0.3 \rightarrow$ use this data to update PM travel time distribution.
- If $0.3 < P(belong\ to\ noon) < 0.7 \rightarrow$ discard the data (because it is too vague to tell which traffic condition this data belongs to).
- Bayesian update

The Bayesian update process is also implemented in WINBUGS. The experiment environment is set the same as in Section 5.2. The convergence of the Markov Chain is guaranteed by checking the chain history and chain autocorrelation function. The posterior means of each parameter are selected to be the new parameters of the travel time distribution. Applying the Bayesian update, the posterior travel time distributions under different traffic conditions, after updating with 75 observations are shown in green curves of Figs. 10 and 11.

• Repetition

Considering the posterior distributions from the previous step as new prior distributions, the traffic condition identification process is performed again on the second half of the data (74 samples). Fig. 12(b) shows the identification results.

The same criteria are applied to classify the data and then the corresponding posterior distributions are updated. Red curves of Fig. 10 and Fig. 11 show the posterior means of each parameter under two traffic conditions (Noon and PM) after updating with all 149 observations.

It can be seen from the figures that if the initial prior distribution is quite accurate such as Fig. 10(c), the posterior distribution doesn't differ very much from the prior. If the initial prior distribution is not so good, such as Fig. 11(a), the

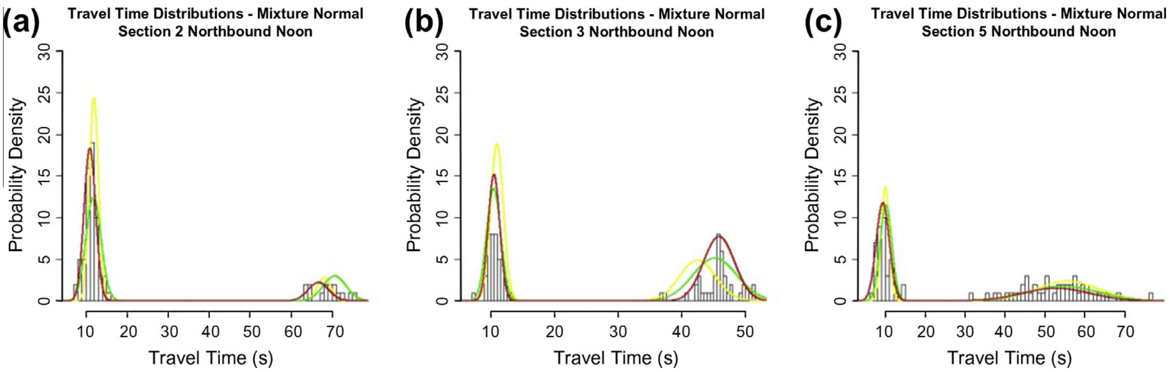

Fig. 10. Comparison among prior and posterior distributions at Noon.

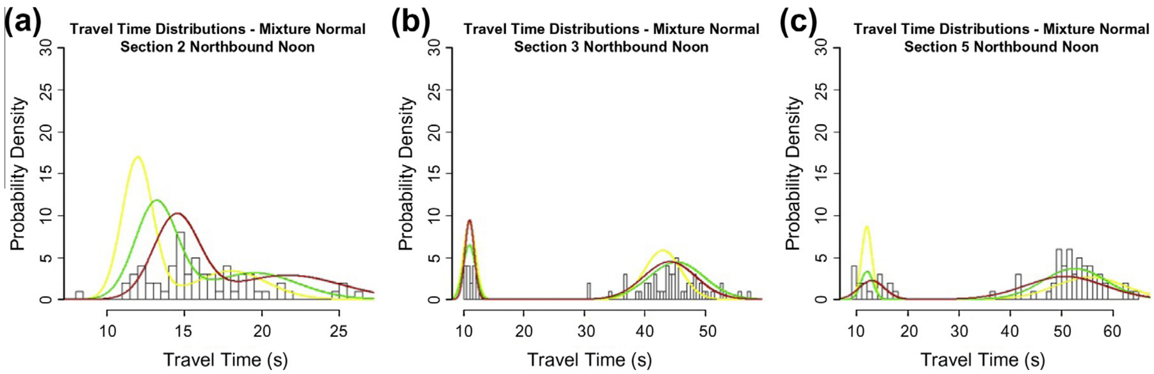

Fig. 11. Comparison among prior and posterior distributions at PM.

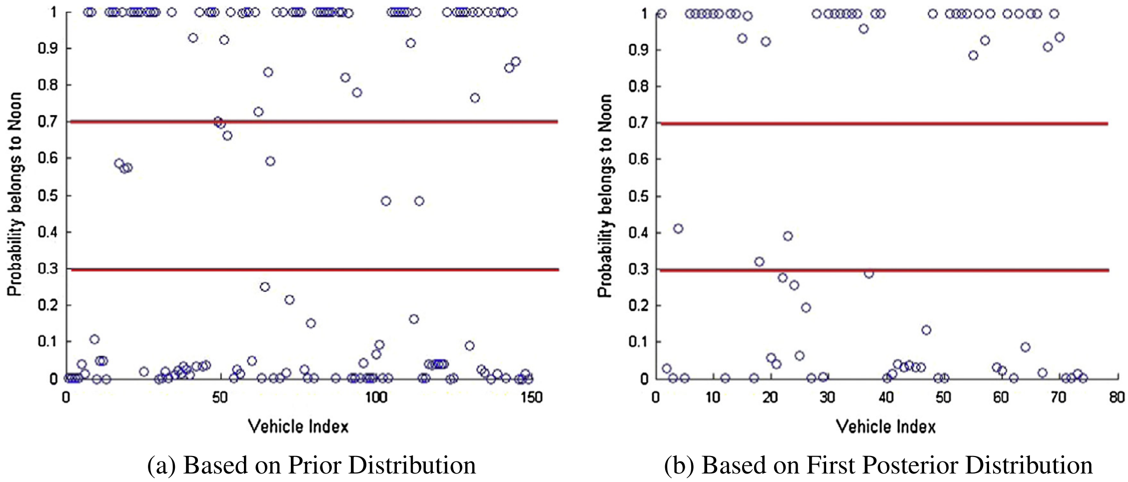

Fig. 12. Data classification.

posterior distribution tends to pull the prior distribution in the right direction. If more data are used to update, then the posterior distribution should become more accurate.

The posterior distributions after updating with all data are compared with results from EM algorithm using the same dataset as shown in Figs. 13 and 14. The red curves represent posterior distribution from Bayesian update and the blue curves represent distributions estimated from EM algorithm.

It can be seen that the Bayesian update and EM algorithm achieved similar results except link 2 at PM (Fig. 14(a)). In this case, the EM algorithm indicates that the two components are separated because there is no data in between. However, the Bayesian posterior distribution says the two components are mixed and the high probabilities between the two components (around 21–24 s) imply some data are missing. If we examine the time space diagram of link 2 at PM as shown in Fig. 15, the Bayesian result is more convincing.

The arterial link between Intersection 1 and Intersection 2 are noted as section 2. If a vehicle passes Intersection 1 at the beginning of green phase at time point *a* and arrives Intersection 2 at time point *b*, it will experience signal delay from time point *b* to time point *d*, which is the end of red phase. If a vehicle passes Intersection 1 at time point *c* and arrives Intersection 2 at time point *d* when the green phase of Intersection 2 just begins, it becomes a non-stopped vehicle. Vehicles passing Intersection 1 between time point *a* and *c* experience signal delay which gradually decreases from a to *c*. In other words, the signal delay time gradually decreases to zero from *d* to *b* and thus there should be no obvious gap between non-stopped and stopped vehicles. The posterior distribution could capture this phenomenon because the Bayesian update combines information not only from data, but also from the prior distribution which is estimated from signal time information.

In addition, Kolmogorov–Smirnov test (Ross, 2009) is run to test the goodness of fit to both EM and Bayesian models. The results are shown in Table 1. Both the D statistic and *p*-value show in all circumstances EM fits the data better than Bayesian update. That is because EM is purely based on the data, while the Bayes estimate also incorporates prior information. EM algorithm used all data while the Bayesian approach discarded some ambiguous data (the posterior probabilities are between 0.3 and 0.7). In addition, the data classification process may put the data into wrong traffic condition. Although

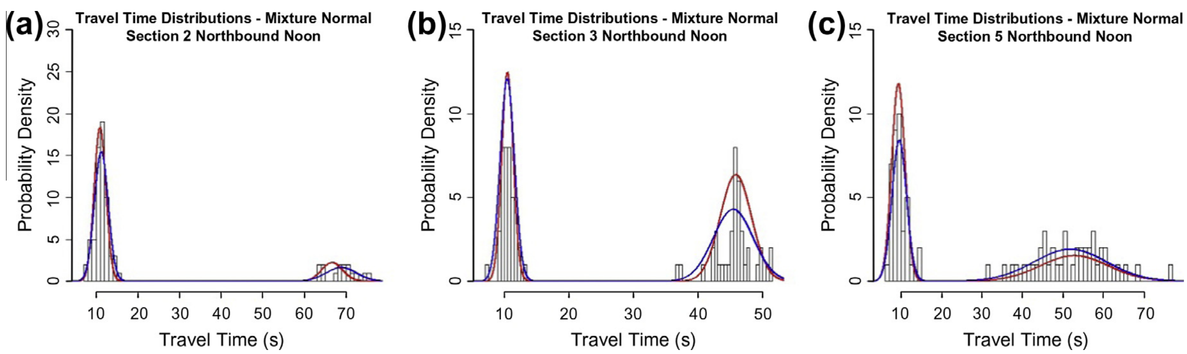

Fig. 13. Comparison between Bayesian update and EM algorithm at Noon.

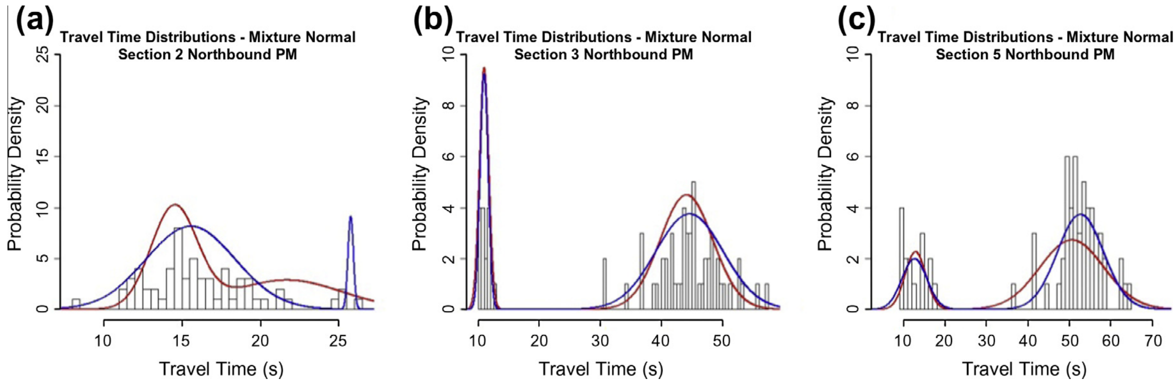

Fig. 14. Comparison between Bayesian update and EM algorithm at PM.

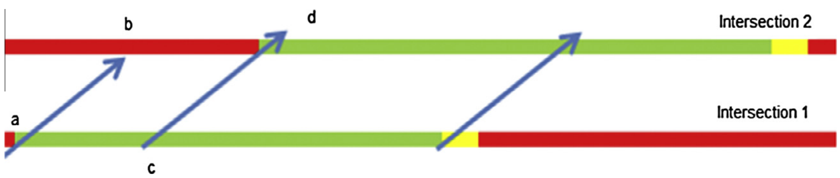

Fig. 15. Time space diagram of link 2 at PM.

Table 1
D-statistic and *p*-value of each section under different traffic condition.

	Section 2 Noon	Section 3 Noon	Section 5 Noon	Section 2 PM	Section 3 PM	Section 5 PM
D statistic						
EM	0.0649	0.0797	0.0613	0.0695	0.0745	0.0807
Bayesian	0.1356	0.0926	0.1303	0.1770	0.1065	0.8079
p-Value						
EM	0.917	0.7211	0.9407	0.9405	0.8772	0.2037
Bayesian	0.1353	0.5344	0.1571	0.0516	0.475	0.0110

the error rate is low, still some data are wrongly updated. However, as stated in the previous paragraph, sometime Bayesian approach could reflect the real world situation when some data is missing while frequentist (EM) did not.

7. A case study – Washington Avenue

In this section, a case study utilizing data collected from GPS vehicles is demonstrated. This case study focuses on one arterial segment of Washington Avenue near the East Bank Campus of University of Minnesota at Twin Cities. The segment includes arterial links on Washington Avenue from Oak Street to the entrance of the Washington Avenue Bridge, in both westbound and eastbound directions as shown in Fig. 16. All links and intersections are labeled by unique identification

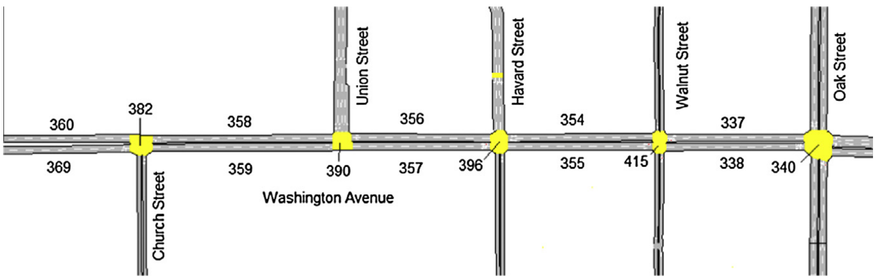

Fig. 16. Washington avenue segment schematic with identification numbers.

numbers. The arterial segment consists of 5 links and intersections in each direction. Of the five intersections, only Intersection 415 is un-signalized.

The GPS travel time data used in this case study was collected to ascertain the traffic flow pattern changes resulting from the opening of the replacement I-35W Mississippi River Bridge in September 2008 (Zhu et al., 2010). GPS devices were installed in commuters' vehicles to track travel time and routes. Most of the participants were staff of the University of Minnesota and they commuted regularly to university for work. The data collection lasted for 13 weeks and more than 2000 link travel times were collected.

Only travel times from through–through vehicles during weekdays are included in this case study. Successive links 369, 359 and 357 are used to construct an eastbound route and links 354, 356 and 358 are used to construct a westbound route. It is assumed that under different signal control plans, traffic conditions are different. Then, three different traffic conditions are defined in this case study: AM rush hour, mid-day and PM rush hour. Each direction of route contains data from two traffic conditions out of the three. The eastbound route contains AM rush hour and mid-day traffic conditions and the westbound route contains PM rush hour and mid-day traffic conditions. The underlying reason is most GPS vehicles came from the Washington Avenue Bridge eastbound and went to the university campus for work in the morning and went back home from university in the evening.

According to the signal-timing plans, periods from 6:00AM to 8:45AM, 8:45AM to 2:45PM, and 2:45PM to 6:15PM constituted the AM, Mid-day, and PM peaks respectively. Then the GPS data was classified into different traffic conditions by their trip times. For eastbound vehicles, 31 GPS travel time sequences were collected during AM rush hour and 23 GPS travel time sequences were collected during mid-day. For westbound vehicles, 30 GPS travel time sequences were collected during PM rush hour and 15 GPS travel time sequences were collected during mid-day.

The travel time distributions are then approximated by mixture normal densities using EM algorithm. The approximated mixture normal distributions for westbound route (link 354, link 356 and link 358) under mid-day and PM rush hour are used. The results are shown in Fig. 17 and Fig. 18 respectively.

The result of real-time traffic condition identification is shown in Fig. 19.

Each dot represents a vehicle. The dots on the left side of the vertical line are the vehicles from mid-day, and on the right side are the vehicles from PM rush hour. The figure shows that the identification result is not accurate for vehicles from mid-day traffic condition. For vehicles from the PM rush hour, most of the time the identification approach can classify the GPS to the right category. The main reason is the sample size of GPS data under mid-day traffic condition is too small. Westbound route under mid-day condition only has 15 samples. It is very difficult to fit a mixture normal model (five parameters) with only 15 samples. The fitted distribution may not reflect the real world scenarios. By contrast, sample size for fitting PM rush

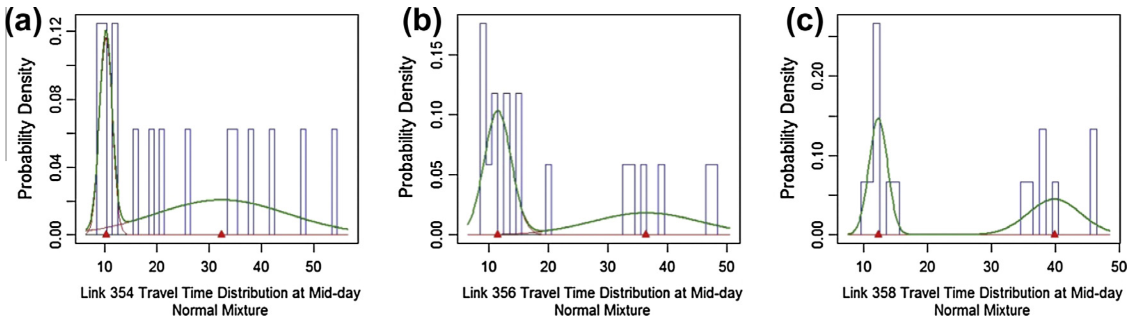

Fig. 17. Normal mixture approximation of westbound travel time (mid-day).

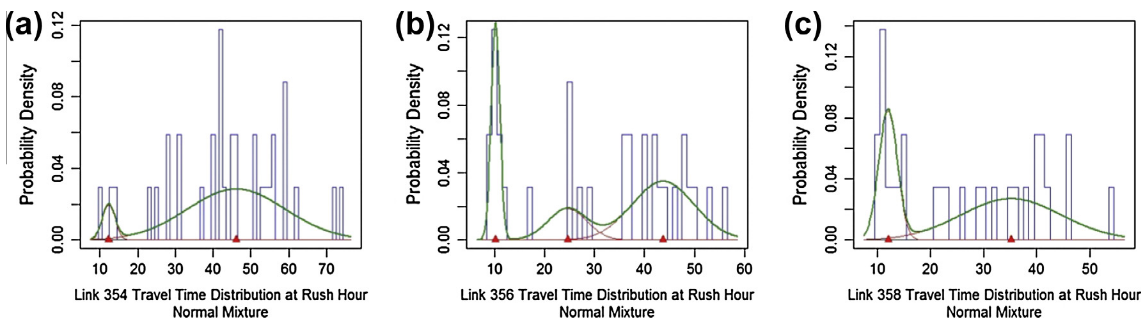

Fig. 18. Normal mixture approximation of westbound travel time (PM rush hour).

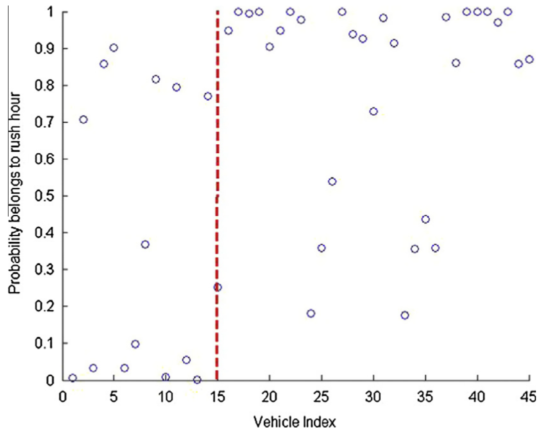

Fig. 19. Traffic condition identification for Washington Avenue GPS Data.

hour traffic condition is larger (30 vehicles) which makes the distribution more accurate. As a result, the identification process could classify more data accurately.

Note that in Fig. 18(b), during rush hour more than two peaks are identified. The third peak represents the vehicles that stopped twice which only happens under an oversaturated condition. Therefore, travel time distributions contain two different traffic conditions: under-saturated (first and second peak) and oversaturated (second and third peak). Travel times from these two traffic conditions need to be further classified. However, if the data are further divided into two parts, the sample size would be too small to fit into a mixture distribution.

The current traffic condition identification approach actually shows the probability of one GPS travel time sequence that belongs to a known traffic condition. However, if a GPS travel time sequence comes from an unknown traffic condition, the current identification approach would be unable to recognize it.

Eq. (14) shows the probability that a GPS travel time sequence belongs to one particular traffic condition is rather a ratio of two probabilities than an actual probability. For example, in Fig. 19, if the ratio is close to one, it means the probability that a GPS travel time sequence belongs to the rush hour distribution is much higher than the probability this sequence belongs to its mid-day counterpart. If a GPS travel time comes from an unknown traffic condition, both the probabilities may be very low. However, the ratio must still be between zero and one. This gives us an initial idea to identify a new traffic condition using actual probabilities. That is, if actual probabilities that belong to all existing traffic conditions are below a threshold, it might suggest this GPS vehicle is from a new traffic condition.

It is shown in Eq. (13) that the probability of a GPS travel time sequence belongs to a certain traffic condition, is the product of the probabilities that each link travel time belongs to each link travel time distribution. Each link probability is calculated as the ratio of probability density of the distribution function. In Washington Avenue case, the route consists of three consecutive links. The threshold of total probability could be set to $0.01 \times 0.01 \times 0.01 = 10^{-6}$. If all of the probabilities is small than the threshold, which means in average all the travel times are beyond the 99th percentile of corresponding distributions, then this GPS data is considered to be from a new traffic condition.

To illustrate this idea, an example based on Washington Avenue westbound GPS data is provided. Fig. 20 shows the results. The value of the Y-axis is the probability after taking $\log_{10}$ of the original probability. Consequently, 10^{-6} is equals to -6 which is the threshold.

The first 45 travel time sequences are either from mid-day or PM rush hour traffic condition. The last two sequences (in the orange circle) are from an unknown traffic condition. The diamond shape indicates that the probability of the travel time

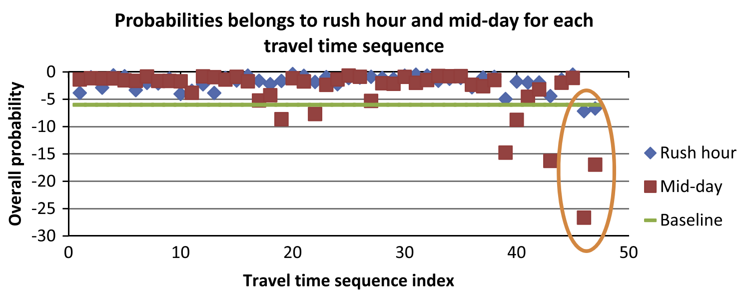

Fig. 20. Experiment on identifying new traffic condition.

belongs to rush hour, and the rectangle shape denotes the probability belongs to mid-day. It can be seen from the figure that for travel time sequences from known traffic conditions, there is no case that both probabilities are below the threshold. However, for the last two travel time sequences, both probabilities are below the threshold which indicates those two travel times come from a new traffic condition.

8. Conclusion remarks and further research

This paper first characterized arterial travel times by probability distributions and defined four travel time states for through–through vehicles. Link travel time distributions were approximated using mixtures of normal densities. According to the definition of travel time states, two approaches to estimate travel time distributions were proposed. If prior travel time data is available, travel time distributions can be estimated empirically, using the EM algorithm. Otherwise, travel time distribution can be estimated based on signal timing information and arterial geometry. Then, GPS travel time data is used to predict the travel time by identifying the traffic condition. The traffic condition identification approach was developed based on Bayes Theorem. Results showed that in most cases, one GPS sample was enough to discriminate between the two traffic conditions. Compared to other approaches, the proposed method needs much less real-time information. Moreover, these GPS data could also be used to update the parameters of the travel time distributions using a Bayesian update. The iterative update process made the posterior travel time distributions more and more accurate. Finally, two comprehensive case studies using the NGSIM Peachtree Street Dataset and GPS and simulation data of Washington Avenue were conducted. The first case study estimated prior travel time distributions based on signal timing and geometric structure under different traffic conditions. Then, travel time data were classified into different traffic conditions and corresponding distributions were updated. In addition, results from the Bayesian update and EM algorithm were compared. Overall, the EM algorithm fit the data better than Bayesian update. However, in some scenarios the Bayesian approach could reflect the real world situation when some data was missing. The second case study first tested the methodologies based on real GPS data to show the importance of sample size. After that, a methodology was proposed to distinguish new traffic conditions.

This paper lays a foundation for the characterization of travel time on urban arterials by probability distributions. Further research could focus on turning vehicles which have more complicated travel time states. Therefore, turning vehicles must necessarily be further divided into sub categories, each category representing only a special scenario of turning. For example, right turn from side streets then go through at the downstream intersection. In addition, estimation of travel time distributions under oversaturated traffic conditions is another interesting topic. When the traffic is in a congested condition and queues can't be fully discharged within one cycle, the bimodal pattern may not be applicable and more travel time states are expected. For example, the vehicles which stopped twice for red signal would generate a new state. Meanwhile, the estimation of travel time based on signal time and geometric structure needs to be modified accordingly.

Acknowledgements

We would like to thank the Intelligent Transportation Systems (ITS) Institute, University of Minnesota, for supporting this project. We would also like to thank the Minnesota Traffic Observatory for hosting this research project providing material and software support. Finally, we would like to acknowledge the importance of the data sets generated and maintained by the NGSIM community. This is one of many research projects these unique datasets have made possible.

References

Berg, B.A., 2004. Markov Chain Monte Carlo Simulations and Their Statistical Analysis: With Web-based Fortran Code. World Scientific, Hackensack, NJ.

Bernardo, J.M., Smith, A.F.M., 2000. Bayesian Theory (Wiley Series in Probability and Statistics), first ed. Wiley.

Boehnke, P., Pfannerstill, E., 1986. System for the automatic surveillance of traffic situations. ITE J. 56.

Box, P., 1976. Manual of Traffic Engineering Studies, forth ed. Institute of Transport. ENGRS, Washington, DC.

Bureau of Public Roads, 1964. Traffic Assignment Manual. U.S. Department of Commerce, Washington, DC.

Cambridge Systematics Inc., 2007. NGSIM Peachtree Street (Atlanta) Data Analysis.

Dailey, Daniel J., Cathey, Fredrick W., 2002. AVL-Equipped Vehicles as Traffic Probe Sensors (Technical Report No. WA-RD 534.1). Washington State Transportation Center (TRAC).

Davis, G.A., Xiong, H., 2007. Access to Destinations: Travel Time Estimation on Arterials (Technical Report No. MnDOT 2007-35 1381). Minnesota Department of Transportation, MN.

DeGroot, M.H., Schervish, M.J., 2002. Probability & Statistics, third ed. Addison-Wesley.

Diebolt, J., Robert, C.P., 1994. Estimation of finite mixture distributions through Bayesian sampling. J. R. Stat. Soc. Ser. B: Methodol. 56, 363–375.

Du, J., 2002. Combined Algorithms for Constrained Estimation of Finite Mixture Distributions with Grouped Data and Conditional Data, Master Thesis. McMaster University.

FHWA, 2006. Next Generation SIMulation Fact Sheet, FHWA-HRT-06-135. <https://www.fhwa.dot.gov/publications/research/operations/its/06135/index.cfm> (accessed 10.10.13).

Gault, H.E., 1981. An on-line measure of delay in road traffic computer-controlled system. Traff. Eng. Control 22.

Geroliminis, N., Skabardonis, A., 2006. Real time vehicle reidentification and performance measures on signalized arterials. In: IEEE Intelligent Transportation Systems Conference, 2006. ITSC '06. Presented at the IEEE Intelligent Transportation Systems Conference, 2006. ITSC '06, pp. 188–193.

Hainen, A.M., Wasson, J.S., Hubbard, S.M.L., Remias, S.M., Farnsworth, G.D., Bullock, D.M., 2011. Estimating route choice and travel time reliability with field observations of Bluetooth probe vehicles. Transp. Res. Rec. J. Transp. Res. Board 2256, 43–50.

Herrera, J.C., Work, D.B., Herring, R., Ban, X. (Jeff), Jacobson, Q., Bayen, A.M., 2010. Evaluation of traffic data obtained via GPS-enabled mobile phones: the Mobile Century field experiment. Transp. Res. Part C Emerg. Technol. 18, 568–583.

Hunter, T., Herring, R., Abbeel, P., Bayen, A., 2009. Path and travel time inference from GPS probe vehicle data. Presented at the Neural Information Processing System foundation (NIPS), Vancouver, Canada.
Liu, H., Ma, W., 2009. A virtual vehicle probe model for time-dependent travel time estimation on signalized arterials. Transp. Res. Part C: Emerg. Technol. 17, 11–26.
Lunn, D., Jackson, C., Best, N., Thomas, A., Spiegelhalter, D.J., 2013. The BUGS Book: A Practical Introduction to Bayesian Analysis.
McLachlan, G., Peel, D., 2000. Finite Mixture Models. John Wiley & Sons, Inc., New York.
McLachlan, G.J., Krishnan, T., 2008. The EM Algorithm and Extensions. Wiley-Interscience, Hoboken, NJ.
National Research Council, 2010. Highway Capacity Manual. Transportation Research Board, Washington.
Nezamuddin, N., Crunkleton, J., Tarnoff, P.J., 2009. Speed distribution profile of traffic data and sample size estimation. Presented at the Transportation Research Board 88th Annual Meeting.
Oppenlander, J.C., 1963. Sample Size Determination for Spot-Speed Studies at Rural, Intermediate, and Urban Locations. Highw. Res. Rec. 35, 78–80.
Ross, S.M., 2009. Introduction to Probability and Statistics for Engineers and Scientists. Academic Press/Elsevier, Amsterdam, Boston.
Skabardonis, A., Dowling, R., 1997. Improved speed-flow relationships for planning applications. Transp. Res. Rec. J. Transp. Res. Board 1572, 18–23.
Spiess, H., 1990. Technical note-conical volume-delay functions. Transp. Sci. 24, 153–158.
Strobel, H., 1977. Traffic Control Systems Analysis by Means of Dynamic State and Input–Output Models (No. A-2361). International Institute for Applied System Analysis, Laxenburg, Austria.
Usami, T., Ikenoue, K., Miyasako, T., 1986. Travel time prediction algorithm and signal operation at critical intersections for controlling travel time. Presented at the Second International Conference on Road Traffic Control, London, United Kingdom, pp. 205–208.
Xie, C., Cheu, R., Lee, D., 2001. Calibration-free arterial link speed estimation model using loop data. J. Transp. Eng. 127, 507–514.
Xiong, H., Davis, G., 2009. Field evaluation of model-based estimation of arterial link travel times. Transp. Res. Rec. J. Transp. Res. Board 2130, 149–157.
Young, C.P., 1988. A relationship between vehicle detector occupancy and delay at signal-controlled junctions. Traff. Eng. Control 29.
Zhang, M., Kwon, E., Wu, T.Q., Sommers, K., Habib, A., 1997. Arterial Link Travel Time Estimation Using Loop Detector Data (Technical Report No. MN/RC - 97/16). MnDOT.
Zhu, S., Levinson, D.M., Liu, H., Harder, K.A., Danczyk, A., 2010. Traffic Flow and Road User Impacts of the Collapse of the I-35W Bridge over the Mississippi River (Technical Report No. Mn/DOT 2010-21). CTS University of Minnesota.